Lateral Aerodynamics of Delta Wings with Leading-Edge Separation

Joseph Katz*
Technion—Israel Institute of Technology, Haifa, Israel

An unsteady vortex-lattice method is presented for the calculation of the aerodynamic forces acting on lifting surfaces undergoing complex three-dimensional motion. For the present case the nonsymmetric motion of a slender delta wing was considered and the resulting lateral characteristics were calculated. The flow separation line was specified along the wing leading edge and the emanating vortex sheet shape and rollup then was calculated. Numerical results are presented for the combined high angle of attack and sideslip condition and for the wing constant roll and coning motions.

Nomenclature

A_f = influence coefficient due to bound circulation
A_s = influence coefficient due to separated wake circulation
A_w = influence coefficient due to trailing-edge circulation
AR = wing aspect ratio
b = wing span
c = wing chord
C_D = drag coefficient
C_L = lift coefficient
$C_{\mathcal{L}}$ = rolling moment coefficient
$C_{\mathcal{L}_\beta}$ = sideslip derivative $\partial C_{\mathcal{L}}/\partial\beta$ (β in degrees)
C_p = pressure coefficient
F = normal force
h = panel vertical distance from x axis
n = vector normal to wing surface
N = number of panels at the wing root
P = pressure
p,q,r = angular velocity about x,y,z axes, respectively
S = wing area
t = time
U = wing forward velocity
u = induced velocity in the x direction
V = panel sideslip velocity
V_p = panel kinematic velocity
v,w = induced velocity in the y and z, directions, respectively
x,y,z = wing coordinates
x_{cg} = location of rotation axis
α = angle of attack
β = sideslip angle
Γ = circulation
Γ_f = wing bound circulation
Γ_s = separated wake circulation
Γ_w = trailing-edge wake circulation
ρ = density
ϕ = velocity potential
ω = wing rate of roll in wind axes

Presented as Paper 82-1386 at the AIAA 9th Atmospheric Flight Mechanics Conference, San Diego, Calif., Aug. 9-11, 1982; submitted Aug. 11, 1982; revision received July 10, 1983.

*Senior Lecturer, Faculty of Mechanical Engineering. Member AIAA.

Introduction

THE low-speed, high-angle-attack aerodynamics of aircraft is of major interest when maneuvers such as short takeoff and landing, or high turning rates are to be considered. The mathematical modeling of the airflow for these conditions becomes rather difficult due to partial or full separation of the lifting surfaces and the time varying flight geometry and wake rollup structure. On the other hand, the ability to control aircraft in these nonlinear situations becomes more desirable, and cases such as short landing on carriers under variable strong side winds or the low-speed sharp turnings will be obtainable. Therefore, the purpose of the present paper is to model the external nonlinear aerodynamics in order to predict aircraft stability derivatives to a future control mechanism.

Current mathematical models of the unsteady aerodynamic response to arbitrary motions of an aircraft are based, for the most part, on the concept of linear stability derivatives. Recent studies extending these mathematical models into the nonlinear aerodynamic regime has been reported in Refs. 1-3. An application of this method for developing a point-by-point control technique for the nonlinear maneuvers will require some prediction method for the linearized coefficients, at each point of the aircraft maneuvers, as noted in these references. A large number of complex unsteady experiments might provide the numerical value for these coefficients; however, their early prediction by some computational scheme is highly desirable.

The present method is an extension of the vortex-lattice method for the calculation of the aerodynamic forces on lifting surfaces undergoing complex three-dimensional unsteady motions. For the present case, the motion of delta wing was considered and the location of separation line was specified along the wing leading edge.

Model

The model presented here assumes that the pressure field around the wing in a low-speed maneuver can be predicted by the potential flow method, if the viscous effects, resulting in some local separations are properly accounted for. These effects, however, are fairly well modeled when the separation line and shed vortex strength is provided to the potential model,[3-6] since vortex motion and wake rollup can then be calculated.

The ability of this concept to predict lift and moment coefficients of highly swept wings up to high angles of attack (with no vortex breakdown) under steady-state conditions is demonstrated by the large spectrum of such works, some of which are quoted in two recent papers.[7,8] The extension of these methods into the unsteady aerodynamic regime occurred

only recently,[3,9-11] whereas only simple motions, such as the wing sudden acceleration or constant rolling with zero angle of attack, were considered. A more general model for the arbitrary three-dimensional motion of wings was proposed by Konstadinopoulos et al.,[12] and the present work is an extension of this approach† to further investigate the lateral aerodynamic characteristics of wings.

It is assumed, therefore, that the flow is incompressible, irrotational, and homogeneous over the fluid region apart from the wing and its wake. Under these conditions a velocity potential ϕ exists, and in an inertial frame of reference the continuity equation becomes

$$\nabla^2\phi=0 \tag{1}$$

The boundary conditions for Eq. (1) require that the wing-induced disturbance will decay far ($|\bar{r}|\to\infty$) from the wing;

$$\nabla\phi=0 \quad \text{for} \quad |\bar{r}|\to\infty \tag{2}$$

and that there will be no flow through the wing surface. This condition, when expressed in a wing-attached coordinate system (as derived in Refs. 4 and 5), yields

$$\nabla\phi\cdot n=\bar{V}_p\cdot n \quad \text{(on the wing)} \tag{3}$$

where $\bar{V}_p$ is the local boundary surface velocity.

Furthermore, for the nonsteady flow, some kind of angular momentum conservation is required, i.e., the overall circulation Γ generated in the fluid must be zero (Kelvin's condition)

$$d\Gamma/dt=0 \quad \text{(for all } t\text{)} \tag{4}$$

To obtain a unique solution of the wing circulation [through Eqs. (1-4)] a smooth tangential flow at the trailing edge is also assumed. This condition is known as the Kutta condition, which requires finite velocities at the trailing edge. In terms of the velocity potential ϕ this condition can be imposed via the formulation

$$\nabla\phi<\infty \quad \text{(at the trailing edge)} \tag{5}$$

To model the viscous effects of the separated flow two additional inputs are required. The first being the location of the separation line. In the present work it is assumed that flow separation is initiated at the delta wing leading edges and therefore this first condition is provided. The second input condition has to determine the strength of the vorticity shed at the leading edges. When potential flow models are to be considered this is possible by the shear velocity method[3,6] or by the assumption used in steady-state vortex-lattice method (VLM) for delta wings,[7,11] as well as in the present work. This latter approach assumes that the bound vortices of the wing separate at the leading edge and then shed into the main flow, or practically each separated vortex line is a continuation of one bound vortex line on the wing surface. The strength of the shedded vorticity, obtained by this method, is most suitable for simulating the flow field above delta wings having sharp leading edges. An inclusion of further viscous effects, such as leading-edge radius or vortex core size, might be considered in a more detailed model.

Once the circulation of the wing and its wake is determined, the calculation of the pressure at any point in the flow is calculated by Bernoulli's equation

$$\frac{P_\infty-P}{\rho}=\frac{1}{2}\left[\left(\frac{\partial\phi}{\partial x}\right)^2+\left(\frac{\partial\phi}{\partial y}\right)^2+\left(\frac{\partial\phi}{\partial z}\right)^2\right]+\frac{\partial\phi}{\partial t} \tag{6}$$

†The details of the present vortex-lattice method differs considerably from the approach taken in Ref. 12.

Vortex-Lattice Solution

The general solution of Eqs. (1-4), according to Green's theorem,[13] consists of a doublet and source distribution over the wing surface. However, for the lifting problem solution, the vortex distribution, which is derived from the doublets, is sufficient. Therefore, the wing planform of Fig. 1 was divided into panels as shown in Fig. 2, and at each panel a vortex ring was placed, as shown in Fig. 3. Also a collocation point [where boundary condition (3) is to be fulfilled] is placed at the panel three-quarter chord at the center of the vortex ring. By selecting the vortex ring representation of Fig. 3, which is a partial solution of Eqs. (1-3) the Kelvin condition is also fulfilled [Eq. (4)]. The placement of the windward vortex element at the panel quarter chord accounts for the Kutta condition. This interpretation was chosen because the velocity induced at a point, far from a two-dimensional wing, can be simulated by placing a single vortex, having the same vorticity, at the wing quarter chord location. The extension of this model, in order to construct a three-dimensional vortex-panel element, was found to be sufficient to satisfy Eq. (5). Then for the complete solution of the problem, in terms of the unknown bound vortices Γ_{f_i}, only boundary condition (3) is left to be solved; i.e., the induced velocity $(\partial\phi/\partial z)_{ij}$ due to the wing vortices and its trailing-edge wake elements Γ_{w_i} and leading-edge wake elements Γ_{s_i} is given at each collocation point by

$$\left(\frac{\partial\phi}{\partial z}\right)_{ij}=[A_{f_{ij}}]\begin{vmatrix}\Gamma_{f_1}\\ \vdots\\ \Gamma_{f_n}\end{vmatrix}+[A_{w_{ij}}]\begin{vmatrix}\Gamma_{w_1}\\ \vdots\\ \Gamma_{w_m}\end{vmatrix}+[A_{s_{ij}}]\begin{vmatrix}\Gamma_{s_1}\\ \vdots\\ \Gamma_{s_1}\end{vmatrix} \tag{7}$$

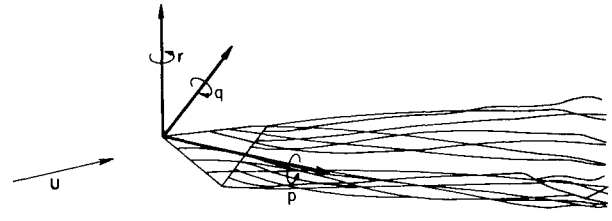

Fig. 1 Schematic of vortex model.

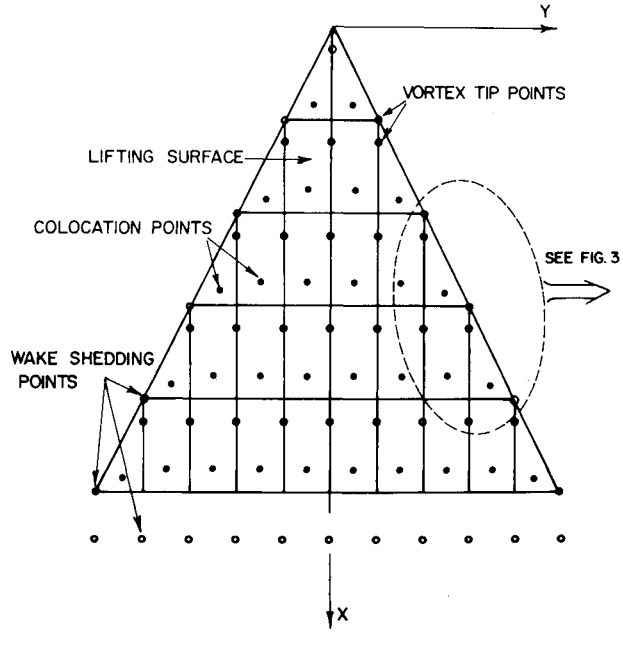

Fig. 2 Geometry of panels on lifting surface (5 × 5 lattice).

Here the influence matrix coefficients $[A_f][A_w]$ and $[A_s]$ are obtained by using the Biot-Savart[13] law for the calculation of the velocities induced by the vortex elements.

The kinematic velocity w_{ij} at each collocation point, due to the wing momentary velocity U, momentary rotation (p,q,r), and camber $z=h(x,y,z)$, is (see Fig. 1):

$$w_{ij} = -\left[(U-ry)\left(\frac{\partial h}{\partial x} - \sin\alpha_i\right) - qx + py + \frac{\partial h}{\partial t}\right] \tag{8}$$

In order to fulfill Eq. (3) the sum of the velocities relative to the panel must be zero

$$w_{ij} + \left(\frac{\partial \phi}{\partial z}\right)_{ij} = 0 \tag{9}$$

and by substituting Eqs. (7) and (8) into Eq. (9), a set of n linear algebraic equations is obtained with the number n of unknown bound vortices Γ_{fi}. The numbers m and l of wake elements in Eq. (7) increase with each time interval and the strength of vortices shed from the trailing edge Γ_{wi} and from the leading edge Γ_{si} are known from previous time steps. If wing geometry does not vary during flight, the matrix $[A_{fij}]$ is calculated only once, whereas the matrices $[A_{wij}]$ and $[A_{sij}]$ are to be calculated at each time step Δt.

Vortex Wake

The modeling of the vortex wake, which is shed at the wing leading and trailing edges, is performed by releasing vortex segments at each time interval Δt (as shown in Fig. 3). This procedure requires a starting-type calculation where at $t=0$ the wing is at rest. Once the wing is suddenly set into motion a vortex segment is shed, as indicated in Fig. 4 (at $t=\Delta t$). Equation (9) is then solved providing the bound circulation distribution on the wing Γ_{fi}. As this calculation is completed the wake deformation is simulated by calculating the downwash $(u,v,w)_i$ at each free-vortex tip and then moving this point according to Eq. (10):

$$\begin{Bmatrix} \Delta x \\ \Delta y \\ \Delta z \end{Bmatrix}_i = \begin{Bmatrix} u \\ v \\ w \end{Bmatrix}_i \Delta t \tag{10}$$

The results of this modeling are shown for various time intervals in Fig. 4, where the wake deformation behind a delta wing which was suddenly set into motion is shown. (Only streamwise vortex wake elements are plotted.) The transient development of the aerodynamic forces (e.g., lift) immediately after the wing was set into motion is reported in Refs. 3 and 4.

Calculation of Aerodynamic Coefficients

When the solution of the circulation distribution [Eq. (9)] is obtained, the pressure difference ΔP_i across each panel is determined by applying the unsteady Bernoulli equation[6]:

$$\Delta P_i = \frac{2\rho}{\Delta s_i}\left[\left(U\int_{x_{i-1}}^{x_i}\frac{\partial\phi}{\partial x}\,dx\right)\Delta y_i + \left(V\int_{y_{i-1}}^{y_i}\frac{\partial\phi}{\partial y}\,dy\right)\Delta x_i + \int_{x_{i-1}}^{x_i}\left(\frac{\partial}{\partial t}\int_0^x \frac{\partial\phi}{\partial x}\,dx\right)dx\Delta y_i\right] \tag{11}$$

Here the velocities U and V are each panel's far-field velocity components due to wing forward flight and rotary motion. Equation (11) can be rewritten in terms of the panel chordwise Γ_{ix} and spanwise Γ_{iy} bound circulation as follows:

$$\Delta F_i = \Delta P_i \Delta s_i = \rho\left[U\Gamma_{i_x}\Delta y + V\Gamma_{i_y}\Delta x + \frac{\partial}{\partial t}\left(\sum_{k=1}^{i-1}\Gamma_{K_x}\Delta x_K + \Gamma_{i_x}\frac{\Delta x_i}{2}\right)\right] \tag{12}$$

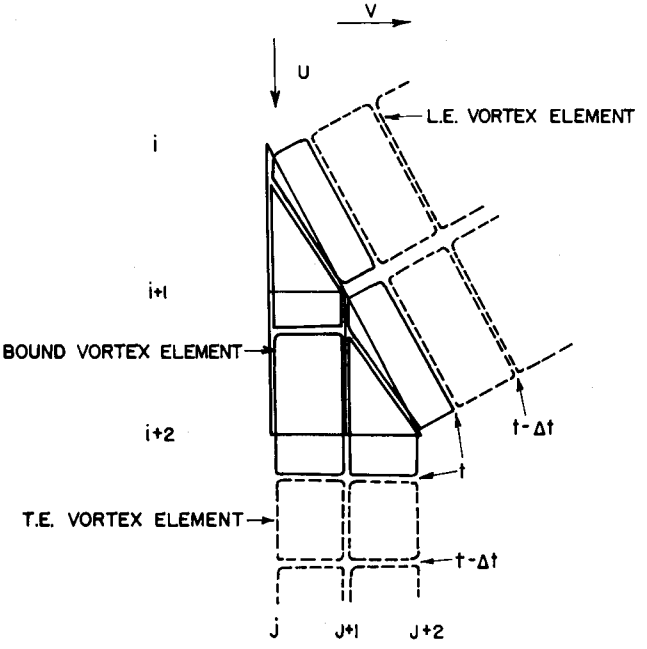

Fig. 3 Vortex-lattice location relative to wing panels.

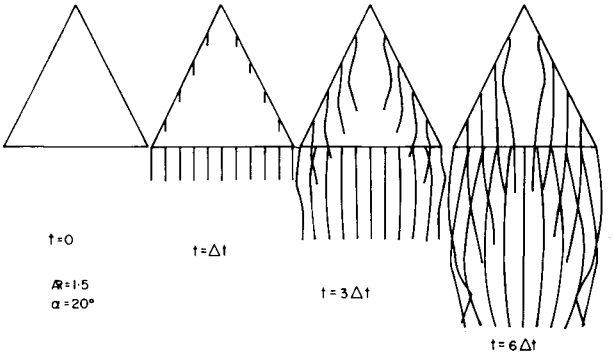

Fig. 4 Vortex wake shedding and rollup sequence.

The resulting lift, drag, pitching moment, and rolling moment coefficients are obtained by integrating each panel normal force ΔF_i along the wing surface.

$$C_L = \sum_{i=1}^{n} \Delta F_i \cos\alpha_i \Big/ \tfrac{1}{2}\rho U^2 S \tag{13}$$

$$C_D = \sum_{i=1}^{n} \Delta F_i \sin\alpha_i \Big/ \tfrac{1}{2}\rho U^2 S \tag{14}$$

$$C_{m_0} = \sum_{i=1}^{n} \Delta F_i x_i \Big/ \tfrac{1}{2}\rho U^2 Sc \tag{15}$$

$$C_{\mathfrak{L}} = \sum_{i=1}^{n} \Delta F_i y_i \Big/ \tfrac{1}{2}\rho U^2 Sb \tag{16}$$

Results

Calculated longitudinal aerodynamic derivatives by the present method were reported in Refs. 3 and 14 where motions such as sudden acceleration and pitch oscillation were considered. In order to model lateral aerodynamic parameters, a vortex lattice for the whole wing (as in Fig. 2) was constructed rather than a half-wing model which was sufficient for longitudinal calculation. Even with this addition, computational effort remained minimal and

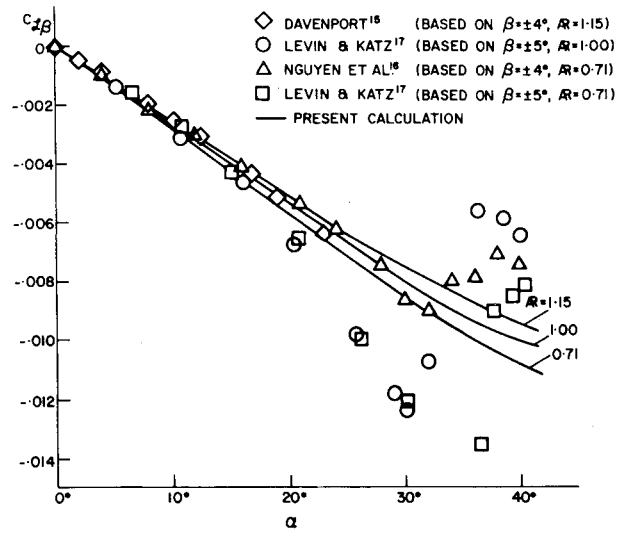

Fig. 5 Variation of lateral-stability derivative with angle of attack and wing aspect ratio.

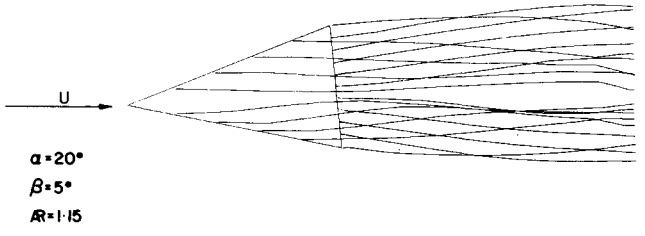

Fig. 6 Wake rollup pattern behind a delta wing (with sideslip).

calculation times for a single point in Fig. 5 (or the situation shown in Fig. 6) were about 80 s on a CDC 7600 computer.

The numerical sensitivity of the above unsteady VLM was proved to be low, since the nonlinear vortex rollup is not calculated by an iterative method.[3] In addition, time interval Δt was kept such that wake element length ($\Delta t \cdot U$) was equal to panel chord (c/N), where N is the number of panels at the wing root,

$$\Delta t = c/NU \tag{17}$$

An increase in panel density, therefore, automatically reduced the time step and resulted in a monotonic improvement in accuracy (e.g., the difference in rolling moment results between a calculation by a 5×5 lattice to the results of a 6×6 lattice were less than 3%, whereas the same difference between the calculations based on an 8×8 and 9×9 lattice were less than 0.1%).

The rolling moment derivative $C_{\mathcal{L}_\beta}$ vs angle of attack α is shown in Fig. 5 ($C_{\mathcal{L}_\beta} = \partial C_{\mathcal{L}}/\partial\beta$, β sideslip, measured in angles) for three wing planforms having $\mathcal{R}=0.71$, 1.0, and 1.15, respectively.

The calculated results are in agreement with some experimental[15-17] data up to $\alpha = 30$-35 deg where the vortex breakdown initiates the wing lift stall. The rolling moments obtained in Ref. 17 are slightly higher than the other data since the wing was centrally mounted on a cylindrical balance. This caused a slight outward displacement of the separated vortex cores, resulting in the above increase in rolling moment derivative.

The calculated wake shape of the model is shown in Fig. 6. Here a vortex lattice of 5×5 was used to model the bound vorticity and a time interval of $\Delta tU/c = 0.2$ served for the wake rollup calculation. Even with this coarse vortex distribution, the rolling moment results and vortex average location compare well with experimental data. Calculated

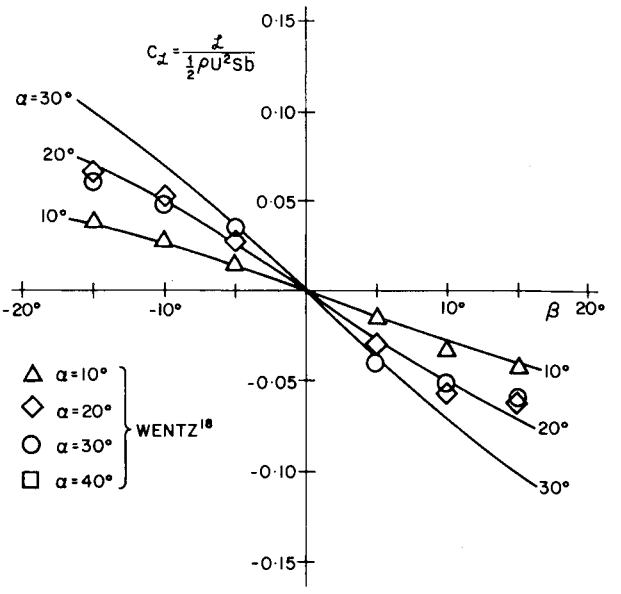

Fig. 7 Effect of sideslip on rolling moment.

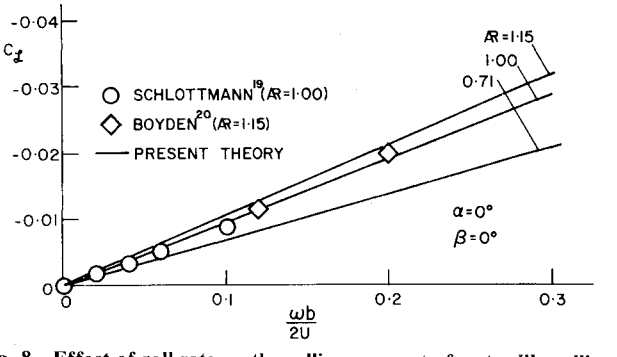

Fig. 8 Effect of roll rate on the rolling moment of a steadily rolling delta wing.

rolling moments as a function of sideslip angle β are presented in Fig. 7 and compared with the experimental results of Wentz.[18] Here as well as in Fig. 5, for angles of attack smaller than $\alpha = 30$ deg and sideslip angles of less than $\beta = 10$ deg, there was a good agreement between calculated and measured data. For higher angles, however, the leeward vortex breaks down and results in a reduction of the rolling moment. This phenomenon is highly complex and cannot be predicted by the present model.

The rolling moment $C_{\mathcal{L}}$ vs the nondimensional roll rate $\omega b/2U$ of three delta wing planforms is shown in Fig. 8. (Here ω is the roll rate in rad/s and b is the full span, $\omega = -p$.) Experimental results of Schlottmann[19] and those extrapolated from Boyden's work[20] are in good agreement with calculated data.

The spanwise pressure distribution at a chord section of $x/c = 0.8$ is shown in Fig. 9. The difference between the calculated data and the measurements of Harvey[21] (and some other analytical models[10,22,23]) can be reduced somewhat by adding more panels to be above the present 5×5 lattice, but the rolling moment will not differ from the values shown in Fig. 8. The wake pattern of a constantly rolling delta wing with a sweepback angle of 80 deg ($\mathcal{R}=0.71$) is shown in Fig. 10. A large time interval of $\Delta tU/c = 0.2$ was used but, even so, the rollup of the two leading-edge vortices is noticeable. Better rollup patterns can be obtained by a further reduction in time intervals; however, this will not result in a difference in rolling moments.

The effect of the roll rate on the wing rolling moment for a coning motion is presented in Fig. 11. Here the wing is rotated

about the axis crossing the trailing edge ($x_{cg}/c = 1.0$) as shown by the insert in Fig. 11. As a result of this motion the leeward leading edge will be subject to sideslip (due to rotation) and the negative rolling moment will increase in magnitude when compared to the rolling moments of Fig. 8.

The effect of rotation axis location on the wing rolling moment is shown by Fig. 12. These rolling moments are measured relative to the wing coordinates as shown in Fig. 1 and not relative to the rotation axis. The right-side insert of Fig. 12 indicates the situation mentioned in the discussion of Fig. 11, whereas the case of rotating the wing about an axis crossing its tip ($x_{cg}/c = 0$) is illustrated in the left insert. In this situation the larger spanwise section of the wing leading edge will gain an additional lift ΔL, resulting in an addition of positive (destabilizing) rolling moment. This effect will increase with an increase in angle of attack and can provide some explanation to airplane instability under similar maneuvers.

Measurement of forces and moments on wings in a non-stationary situation is extremely difficult and experimental data is minimal. Recently, however, Nguyen et al.[16] published such results and they are presented in Fig. 13. A comparison of these results for two angles of attack ($\alpha = 10$ and 20 deg) shows a major difference in the slope of these curves and some nonlinear behavior is to be expected. It is encouraging, therefore, that the calculated results of the present com-

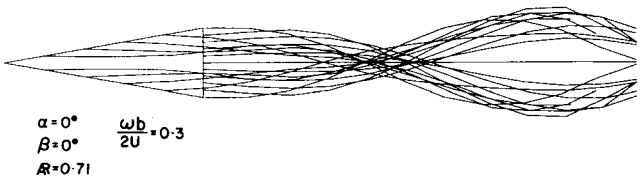

Fig. 10 Wake rollup pattern behind a delta wing in a constant rolling motion.

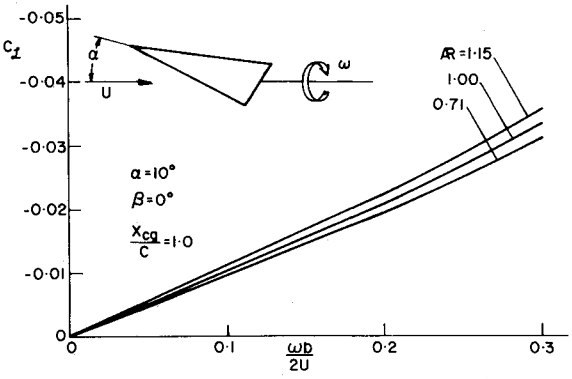

Fig. 11 Effect of roll rate on the rolling moment of a delta wing undergoing a coning motion.

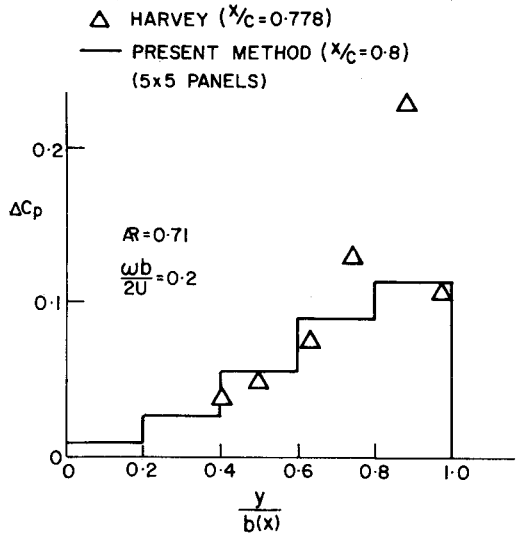

Fig. 9 Spanwise pressure-difference distribution on a steadily rolling delta wing.

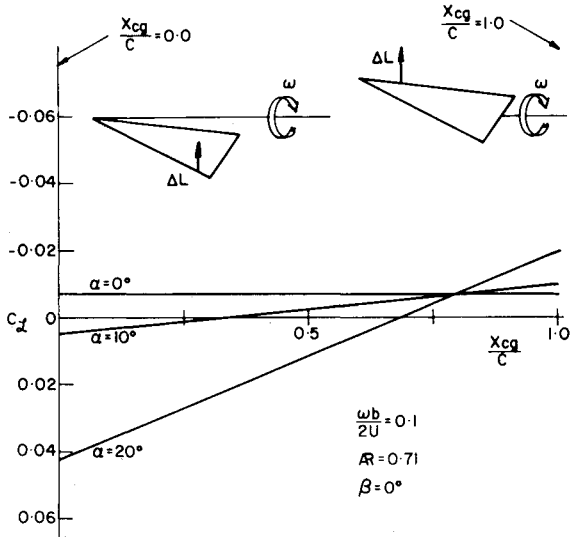

Fig. 12 Effect of rotation axis location on the rolling moment of a delta wing in a coning motion.

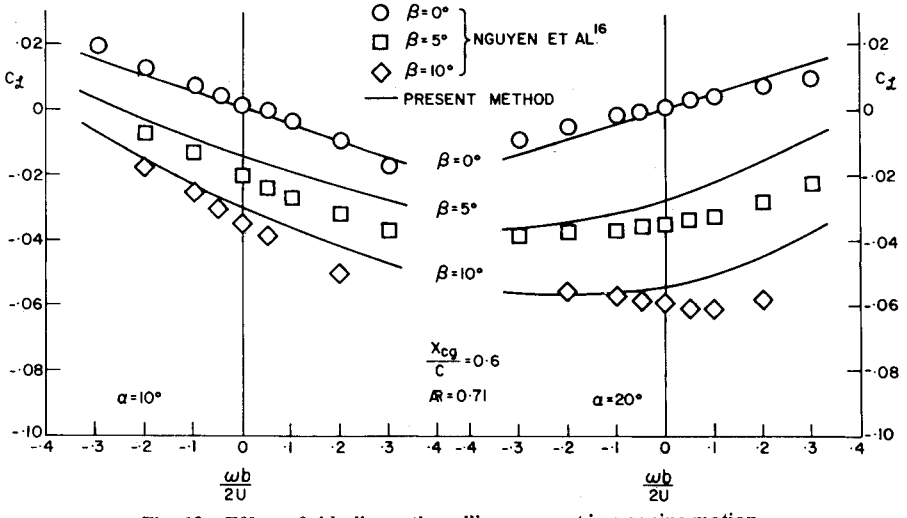

Fig. 13 Effect of sideslip on the rolling moment in a coning motion.

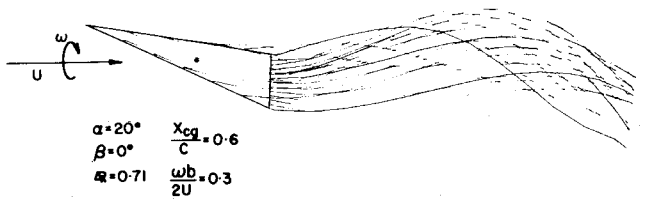

Fig. 14 Wake rollup pattern behind a delta wing undergoing a coning motion

putational method compare so well with this data. The reason for this inversion in the curves slope is purely kinematical and it is a result of the effect shown in Fig. 12.

At an angle of attack of $\alpha = 10$ deg the curve slope of the pure rotational mode ($\alpha = 0$ deg) is maintained in a manner indicated by Fig. 8. When increasing angle of attack up to $\alpha = 20$ deg, a positive addition to the rolling moment will take place as suggested by Fig. 12 ($x_{cg}/c = 0.6$). An increase in rotation speed will increase this effect more than the negative moments of the pure rotation and the combined situation will result in an overall positive gradient of these curves.

Wake rollup pattern behind a delta wing undergoing a coning motion is shown in Fig. 14. The rotation axis here is across $x_{cg}/c = 0.6$, according to the data shown in Fig. 13. Time intervals used here are similar to those used for Figs. 6 and 10 and for this case. A reduction in time interval also did not affect the values of calculated rolling moments.

Conclusions

The vortex-lattice model presented here enabled the calculation of aerodynamic forces acting on a delta wing undergoing a complex three-dimensional motion. The transition from stabilizing to destabilizing rolling moments in a coning motion was calculated and found to compare well with existing experimental data. The possibility of calculating these forces can improve our understanding of the aerodynamic forces during aircraft spin and pre-stall/spin conditions and thus contribute to aircraft safety.

The primary effort of this work was to develop and solve the kinematical problem associated with the complex three-dimensional motion of the wing planform. Therefore, standard methods were used for the subdivision of the wing into panels and vortex elements and for wake rollup calculation. Even so, the integral results, such as forces and moments, were satisfactory, whereas pressure distribution on the wing surface was not finely detailed. Thus, a logical development of this work would include improvements both in vortex panel shapes and numbers and should improve the simulation of separated vortex wake rollup.

Acknowledgments

The work presented herein was supported under NASA Grant NAGW-00218 with Dr. Lewis B. Schiff as project monitor.

References

[1] Tobak, M. and Schiff, L. B., "A Nonlinear Aerodynamic Moment Formulation and its Implications for Dynamic Stability Testing," AIAA Paper 71-275, 1971.

[2] Tobak, M. and Schiff, L. B., "Nonlinear Aerodynamics of Aircraft in High-Angle-of-Attack Maneuvers," AIAA Paper 74-85, 1974.

[3] Levin, D. and Katz, J., "Vortex-Lattice Method for the Calculation of the Nonsteady Separated Flow over Delta Wings," *Journal of Aircraft*, Vol. 18, Dec. 1981, pp. 1032-1037.

[4] Katz, J., "Method for Calculating Wing Loading During Maneuvering Flight Along a Three Dimensional Curved Path," *Journal of Aircraft*, Vol. 16, Nov. 1979, pp. 739-741.

[5] Katz, J., "A Discrete Vortex Method for the Nonsteady Separated Flow over an Airfoil," *Journal of Fluid Mechanics*, Vol. 102, Jan. 1981, pp. 315-328.

[6] Katz, J., "Large Scale Vortex Lattice Model for the Locally Separated Flow over Wings," *AIAA Journal*, Vol. 20, Dec. 1982, pp. 1640-1646.

[7] Johnson, F. T. and Tinoco, E. N., "Recent Advances in the Solution of Three-Dimensional Flows over Wings with Leading Edge Vortex Separations," AIAA Paper 79-0282, 1979.

[8] Lamar, J. E. and Luckring, J. M., "Recent Theoretical Developments and Experimental Studies Pertinent to Vortex Flow Aerodynamics with a View Toward Design," AGARD CP-247, Oct. 1978.

[9] Atta, E. H., Kandil, O. A., Mook, D. T., and Nayfeh, A. H., "Unsteady Aerodynamic Loads on Arbitrary Wings Including Wing-Tip and Leading-Edge Separation," AIAA Paper 77-156, 1977.

[10] Kandil, O. A., Atta, E. H., and Nayfeh, A. H., "Three Dimensional Steady and Unsteady Asymmetric Flow Past Wings of Arbitrary Planforms," AGARD CP-227, Sept. 1977.

[11] Kandil, O. A., "State of Art of Nonlinear Discrete-Vortex Methods for Steady and Unsteady High Angle of Attack Aerodynamics," AGARD CP-247, 1978.

[12] Konstandinopoulos, P., Mook, D. T., and Nayfeh, A. H., "A Numerical Method for General, Unsteady Aerodynamics," AIAA Paper 81-1877, 1981.

[13] Robinson, A. and Laurmann, J. A., *Wing Theory*, Cambridge University Press, Cambridge, England, Chap. 1, 1956.

[14] Levin, D., "A Vortex Lattice Method for Calculating Longitudinal Dynamic Stability Derivatives of Oscillating Delta Wings," AIAA Paper 81-1876, 1981.

[15] Davenport, E. E. and Huffman, J. K., "Experimental and Analytical Investigation of Subsonic Longitudinal and Lateral Aerodynamic Characteristics of Slender Sharp-Edge 74° Swept Wings," NASA TN D-6344, July 1971.

[16] Nguyen, L. T., Yip, L., and Chambers, J. R., "Self-Induced Wing Rock of Slender Delta Wings," AIAA Paper 81-1883, Aug. 1981.

[17] Levin, D. and Katz, J., "Dynamic Load Measurement of Delta Wings Undergoing Self-Induced Roll Oscillations," AIAA Paper 82-1320, Aug. 1982.

[18] Wentz, W. H. Jr., "Effects of Leading Edge Camber on Low-Speed Characteristics of Slender Delta Wings," NASA CR-2002, Oct. 1972.

[19] Schlottmann, F., "The Steady and Unsteady Aerodynamic Coefficients for the Rolling Motion of Slender Wings," Ph.D. Dissertation Ruhr University, Bochum, W. Germany, 1972.

[20] Boyden, R. P., "Effects of Leading-Edge Flow on the Roll Damping of Slender Wings," *Journal of Aircraft*, Vol. 8, Aug. 1971, pp. 543-547.

[21] Harvey, J. K., "A Study of the Flow Field Associated with a Steadily-Rolling Slender Delta Wing," *Journal of the Royal Aeronautical Society*, Vol. 68, Feb. 1964, pp. 106-110.

[22] Hanin, M. and Mishne, D., "Flow about a Rolling Slender Wing with Leading Edge Separation," *Israel Journal of Technology*, Vol. 11, No. 3, 1973, pp. 131-136.

[23] Cohen, M. J. and Nimri, D., "Aerodynamics of Slender Rolling Wings at Incidence in Separated Flow," *AIAA Journal*, Vol. 14, July 1976, pp. 886-893.